Spine

SPINE Volume 38, Number 2, pp E84–E93
©2013, Lippincott Williams & Wilkins

BIOMECHANICS

ProDisc Cervical Arthroplasty Does Not Alter Facet Joint Contact Pressure During Lateral Bending or Axial Torsion

Nicolas V. Jaumard, PhD,* Joel A. Bauman, MD,* Benjamin B. Guarino, BS,† Akhilesh J. Gokhale, MS,‡ Daniel E. Lipschutz, BS,† Christine L. Weisshaar, MS,*† William C. Welch, MD,* and Beth A. Winkelstein, PhD*†

Study Design. A biomechanical study of facet joint pressure after total disc replacement using cadaveric human cervical spines during lateral bending and axial torsion.

Objective. The goal was to measure the contact pressure in the facet joint in cadaveric human cervical spines subjected to physiologic lateral bending and axial torsion before and after implantation of a ProDisc-C implant.

Summary of Background Data. Changes in facet biomechanics can damage the articular cartilage in the joint, potentially leading to degeneration and painful arthritis. Few cadaveric and computational studies have evaluated the changes in facet joint loading during spinal loading with an artificial disc implanted. Computational models have predicted that the design and placement of the implant influence facet joint loading, but limited cadaveric studies document changes in facet forces and pressures during nonsagittal bending after implantation of a ProDisc. As such, little is known about the local facet joint mechanics for these complicated loading scenarios in the cervical spine.

Methods. Seven osteoligamentous C2–T1 cadaveric cervical spines were instrumented with a transducer to measure the C5–C6 facet pressure profiles during physiological lateral bending and axial torsion, before and after implantation of a ProDisc-C at that level. Rotations at that level and global cervical spine motions and loads were also quantified.

Results. Global and segmental rotations were not altered by the disc implantation. Facet contact pressure increased after implantation during ipsilateral lateral bending and contralateral torsion, but that increase was not significant compared with the intact condition.

Conclusion. Implantation of a ProDisc-C does not significantly modify the kinematics and facet pressure at the index level in cadaveric specimens during lateral bending and axial torsion. However, changes in facet contact pressures after disc arthroplasty may have long-term effects on spinal loading and cartilage degeneration and should be monitored *in vivo*.

Key words: disc arthroplasty, cervical spine, biomechanics, facet joint, contact pressure. **Spine 2013;38:E84–E93**

Coupling between axial torsion and lateral bending enables the complex motions required for the normal biomechanical function of the cervical spine.[1–9] The oblique orientation of the cervical facets in the sagittal and coronal planes contributes to this coupling and to load transmission while guiding and restricting spinal motions.[10–12] The facet and Luschka joints contribute to cervical stability and coupling.[13–15] Although anatomical and biomechanical studies suggest that the articular cartilage of the facet joint is subjected to complex mechanical loading,[16,17] few studies have quantified the local loading in this joint.[18–20]

Facet cartilage loading is not uniform and is modified by changes in spinal kinematics resulting from trauma, degeneration, and/or surgical intervention.[20–26] Consequently, any change in facet joint biomechanics can alter the structural integrity and health of this joint's articular cartilage and can potentially lead to its degeneration and painful arthritic changes.[27–34] Total disc replacement restores the segmental motion of the spine.[35–40] However, clinical investigations have reported potential complications in the spine at follow-up, such as facet arthrosis.[41–44] Both cadaveric and computational studies report varied facet forces depending on the loading, the position, and type of implant and the spinal region.[45–54] Finite element models predict an increase in lumbar facet force during both flexion and extension.[49,55,56] In contrast, a computational model predicted that facet forces decrease after implantation of a semiconstrained disc implant but increase with an unconstrained implant that allows more flexibility.[52] Anterior placement of a lumbar artificial disc increases facet

From the Departments of *Neurosurgery; †Bioengineering; and ‡Mechanical Engineering & Applied Mechanics, University of Pennsylvania, Philadelphia, PA.

Acknowledgment date: July 18, 2012. First revision date: September 20, 2012. Second revision date: October 25, 2012. Acceptance date: October 28, 2012.

The device(s)/drug(s) is/are FDA approved or approved by corresponding national agency for this indication.

Synthes, Inc., the Catharine Sharpe Foundation, and a Research Fellowship from the Neurosurgery Research & Education Foundation funds were received to support this work.

Relevant financial activities outside the submitted work: grants, expert testimony, patent.

Address correspondence and reprint requests to Beth A. Winkelstein, PhD, Department of Bioengineering, School of Engineering and Applied Science, University of Pennsylvania, 210 S. 33rd St, Room 240 Skirkanich Hall, Philadelphia, PA 19104; E-mail: winkelst@seas.upenn.edu

DOI: 10.1097/BRS.0b013e31827b8a2d

loads during compression and extension,[45,49] whereas the anteroposterior position of an artificial disc does not influence facet forces in the cervical spine.[53]

A very limited number of studies have evaluated facet loading during the more complicated lateral bending and axial torsion regimes. Finite element models of lumbar motion segments predict a substantial increase in facet load after ProDisc-L arthroplasty.[49,55] In contrast, Kang *et al*[52] reported a 40% lower facet force in lateral bending after ProDisc-C arthroplasty than in the intact condition using a finite element model. Computational models of lumbar and cervical motion segments predict that a posterior placement, a small ball radius, and a low or high center of rotation of a ball-and-socket–type implant increase facet forces in lateral bending and axial torsion.[50,53] However, few cadaveric studies have evaluated the effect of the ProDisc on facet joint loading during lateral bending and axial torsion. Flexible intra-articular sensors detected an increase in lumbar facet force on the ipsilateral side during lateral bending after disc replacement at L5–S1.[46] Yet, strain gauges implemented on the facet surfaces of cervical spines measured a decrease in facet force in lateral bending and axial torsion after ProDisc-C implantation compared with the intact condition.[47] Despite these estimations of facet forces developed during complex nonsagittal loading before and after disc arthroplasty, quantitative measurements of the contact pressure that develops in the human cervical facet joints are still lacking.

The objective of this study was to measure the pressure profile in the cervical facet joint of cadaveric cervical spines during lateral bending and axial torsion to investigate the influence of single level ProDisc-C arthroplasty on local facet joint mechanics at the index level. Using a minimally invasive technique previously described,[54,57] the C5–C6 facet pressure was measured in multisegment cadaveric cervical spines under physiological conditions of lateral bending and axial torsion toward and away from the instrumented facet joint. Biomechanical outcomes were compared between the intact and implanted conditions to evaluate the effect of disc arthroplasty on facet joint loading.

MATERIALS AND METHODS

Seven fresh-frozen male cadaveric spines from C2 to T1 (age range, 37–78 yr; mean, 60 ± 13 yr) were evaluated by fluoroscopy and the degenerative state of the disc and facets of each specimen was graded according to customary procedures.[58,59] The 2 oldest age specimens (ages, 69 and 78 yr) were evaluated as exhibiting a minimal and moderate disc degeneration at C5–C6, respectively; the remaining 5 younger specimens exhibited no signs of disc degeneration. Crossed Kirschner wires were placed in each of the C2 and T1 vertebrae to rigidly fix the specimen to aluminum cups using potting material (FlowStone; Whip Mix Corp., Louisville, KY). Three reflective beads (6.35-mm diameter) were attached to the lateral masses and anterior face of each vertebral body and also to the casting cups for motion tracking during testing (Figure 1). A tip-mounted pressure transducer (XCEL-100-50A; Kulite, Leonia, NJ) was inserted in the left C5–C6 facet joint to measure the contact pressure, using a previously validated noninvasive approach.[26,57] The pressure sensor was positioned through a hole drilled in the posterior aspect of the left C5 lateral mass to contact the C6 articular surface (Figure 2).[26,54,57]

Each cervical spine specimen was rigidly fixed to a 6-axis load cell (Model 4386; RA Denton Inc., Rochester Hills, MI) in a testing frame by the T1 casting cup (Figure 1). A moment arm was attached to the top of the C2 cup to apply lateral bending and axial torsion separately. A cable was attached to one end of the moment arm to apply lateral bending toward (ipsilateral; left) or away from (contralateral; right) the side with the pressure probe. Similarly, cables were connected to each end of the moment arm to apply ipsilateral and contralateral torsion directed toward and away from the left side. Pneumatic pistons attached to the cables imposed lateral bending and axial torsion moments of 3.0 N·m and 2.7 N·m, respectively.[47,60,61] The combined weight of the C2 casting cup, potting material, and moment arm applied a compressive preload of 14 N, which did not induce any extension or flexion.[57] An optical system of 4 infrared cameras (PEAK Motus 8.0; Vicon, Denver, CO) tracked the position of the reflective beads at 120 Hz, and image data were synchronized with the load and pressure data that were acquired at 600 Hz.

All specimens were imaged with 3-dimensional fluoroscopy after implantation to assess whether proper implant position was obtained. In the sagittal slice image showing the keels of the implant, the distance between the posterior edge of the implant and the line joining the posterior edges of the adjacent upper and lower vertebral bodies was measured at the midheight of the disc.

Prior to testing, specimens were preconditioned by manual exercise through several cycles of bending and torsion. Lateral bending and axial torsion were then applied to intact specimens in a randomized order. Following that loading protocol, a ProDisc-C (Synthes, West Chester, PA) was implanted at C5–C6 using standard operative techniques including a minimal bilateral uncinectomy and complete posterior longitudinal ligament removal.[54] Trial discs were used to select the implant size (*i.e.*, height, depth, width) that best fits each specimen. Four different implant footprints were used (medium, medium deep, large, large deep), but 6 of the 7 implants had a height of 5 mm and 5 implants had a width of 17 mm, with the depths ranging from 12 to 16 mm, as previously described.[54] The lateral bending and axial torsion loading protocols were then repeated on the implanted specimens in randomized order.

Changes in the forces, moments, and pressures in the C5–C6 joint during loading were used to calculate the primary and coupled motions and loads. The global (C2–T1) and segmental vertebral motions at the index level (C5–C6) were also measured. All mechanical data were acquired in both the intact and the implanted (ProDisc) conditions during both ipsilateral and contralateral lateral bending and

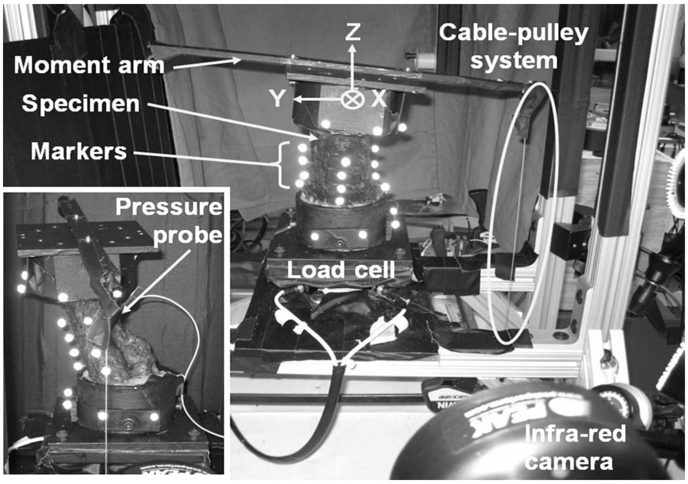

Figure 1. Anterior and lateral (insert) views of a specimen in the loading frame with the load cell and cable pulley system with cable (circled) attached to the moment arm. Also shown are the reflective markers and the infrared tracking cameras. In this configuration, the setup is assembled to apply left (ipsilateral) lateral bending in the direction of the probe placed in the left C5–C6 facet joint.

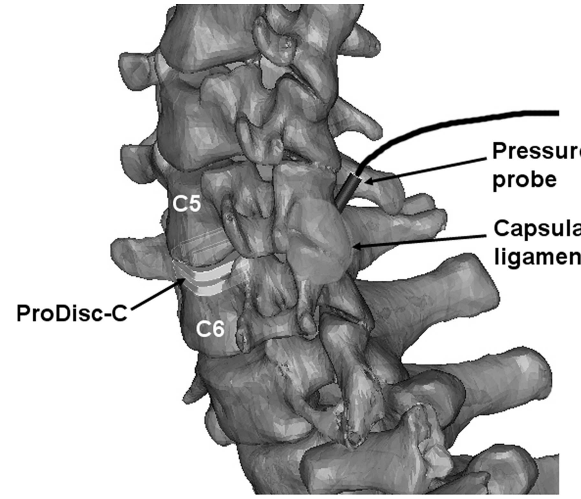

Figure 2. Three-dimensional rendering of a cervical spine specimen showing the ProDisc-C at C5–C6 and the pressure probe inserted in the left C5–C6 facet joint. A semitransparent capsular ligament has been added in this rendering covering the left C5–C6 facet joint.

axial torsion. The maximum changes in forces (ΔF) and moments (ΔM) were calculated as the difference between the initial and maximum moments during the loading phase (Figure 3). Similarly, the maximum global ($\Delta\theta_G$) and segmental ($\Delta\theta_S$) rotations were calculated as this same difference in angular positions during the loading phase, as was the maximum change in facet pressure (ΔP). Coupling was also evaluated using the primary and coupled rotations. For lateral bending, these rotations were about the *x*-axis and *z*-axis, respectively (Figure 1); for axial torsion, they were about the *z*-axis and *x*-axis, respectively. In lateral bending, the ratios of coupled-to-primary rotations were determined as $\Delta\theta_{G\text{-}AT}/\Delta\theta_{G\text{-}LB}$ and $\Delta\theta_{S\text{-}AT}/\Delta\theta_{S\text{-}LB}$ and in axial torsion the ratios were $\Delta\theta_{G\text{-}LB}/\Delta\theta_{G\text{-}AT}$ and $\Delta\theta_{S\text{-}LB}/\Delta\theta_{S\text{-}AT}$. All ratios were expressed as percentages.

Comparisons were made between the intact and implanted conditions for ipsilateral and contralateral lateral bending and axial torsion. Changes in primary and coupled moments were compared for each of the ipsilateral and contralateral directions and for each of lateral bending and axial torsion using paired *t* tests. The change in primary and coupled moments (ΔM_x, ΔM_z), compressive force (ΔF_z), global ($\Delta\theta_{G\text{-}LB}$, $\Delta\theta_{G\text{-}AT}$) and segmental ($\Delta\theta_{S\text{-}LB}$, $\Delta\theta_{S\text{-}AT}$) angles, and facet pressure (ΔP) was compared between the intact and implanted conditions using analysis of variance with repeated measures for ipsilateral and contralateral loading, for each of lateral bending and axial torsion, separately. The ratios of coupled-to-primary moments and rotations were also compared between the intact and implanted conditions, with repeated measures analysis of variances. The changes in primary moment, primary global and segmental angles, and facet pressure were also compared between the ipsilateral and contralateral directions for both loading modes in both the intact and implanted conditions using analysis of variances.

RESULTS

The artificial discs were positioned anterior to the spinal canal at an average distance of 1.7 ± 1.7 mm. Similar forces and moments were applied to the specimens before and after implantation of the ProDisc-C in both lateral bending and axial torsion (Figure 4; Table 1). The increase in compressive force (ΔF_z) induced by either type of loading in both the intact and implanted conditions was small and under 8 N in lateral bending and under 4 N in axial torsion. The increase in the coupled forces in the axial plane (ΔF_x, ΔF_y) was also small (<3 N) in both loading modes (Figure 4; Table 1).

The changes in primary and coupled moments were comparable between the intact and implanted conditions for both loading directions (Figures 3 and 4; Table 1). In lateral bending, the change in primary moment was similar between the intact and implanted conditions for both the ipsilateral (intact: 2.9 ± 0.6 N·m; implanted: 3.3 ± 0.9 N·m) and contralateral (intact: −3.3 ± 0.9 N·m; implanted: −2.9 ± 0.6 N·m) directions. There was no difference between the ipsilateral and contralateral ΔM_x values that were significantly greater ($P < 0.001$, power = 100%) than the changes in coupled moments, ΔM_z and ΔM_y, for each of the conditions in lateral bending (Figure 4; Table 1). The change in torsion moment was similar between both conditions for ipsilateral torsion (intact: 2.6 ± 0.5 N·m; implanted: 2.8 ± 0.3 N·m) but not for contralateral torsion when it was significantly increased ($P = 0.003$, power = 35.5%) (Figure 4). There was no difference between the ipsilateral and contralateral ΔM_z moments, which were significantly greater ($P < 0.001$, power = 100%) than the changes in the coupled moments for each of the intact and implanted conditions in torsion (Figure 4; Table 1).

The global and segmental rotations were similar for all cases in lateral bending and torsion (Figure 4; Table 1). The change in primary global angle ($\Delta\theta_{G\text{-}LB}$) was similar between the intact and implanted conditions for ipsilateral and

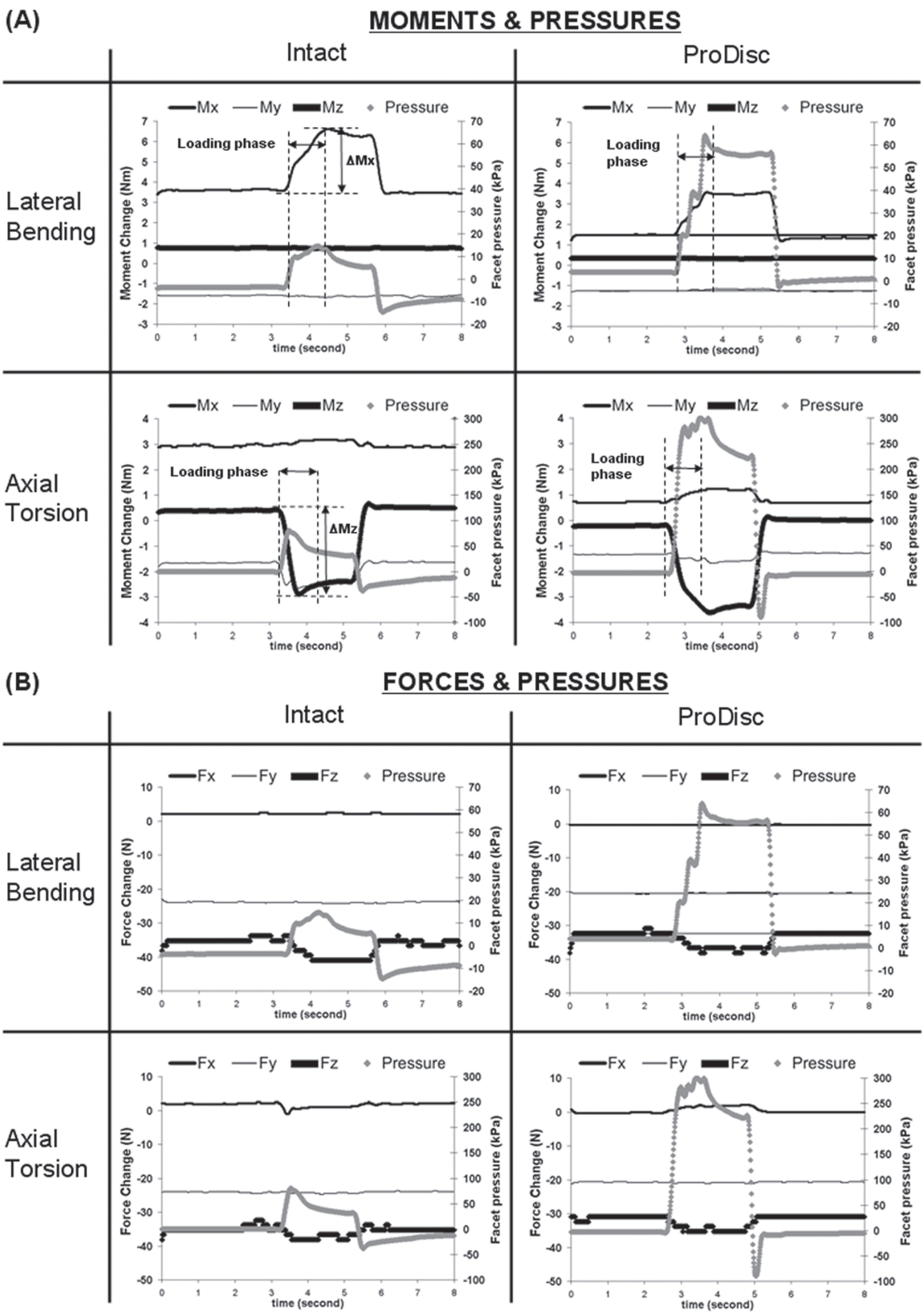

Figure 3. Temporal traces of the moments and facet pressures **(A)** and forces and facet pressures **(B)** for ipsilateral lateral bending and contralateral axial torsion for both the intact and implanted (ProDisc) conditions.

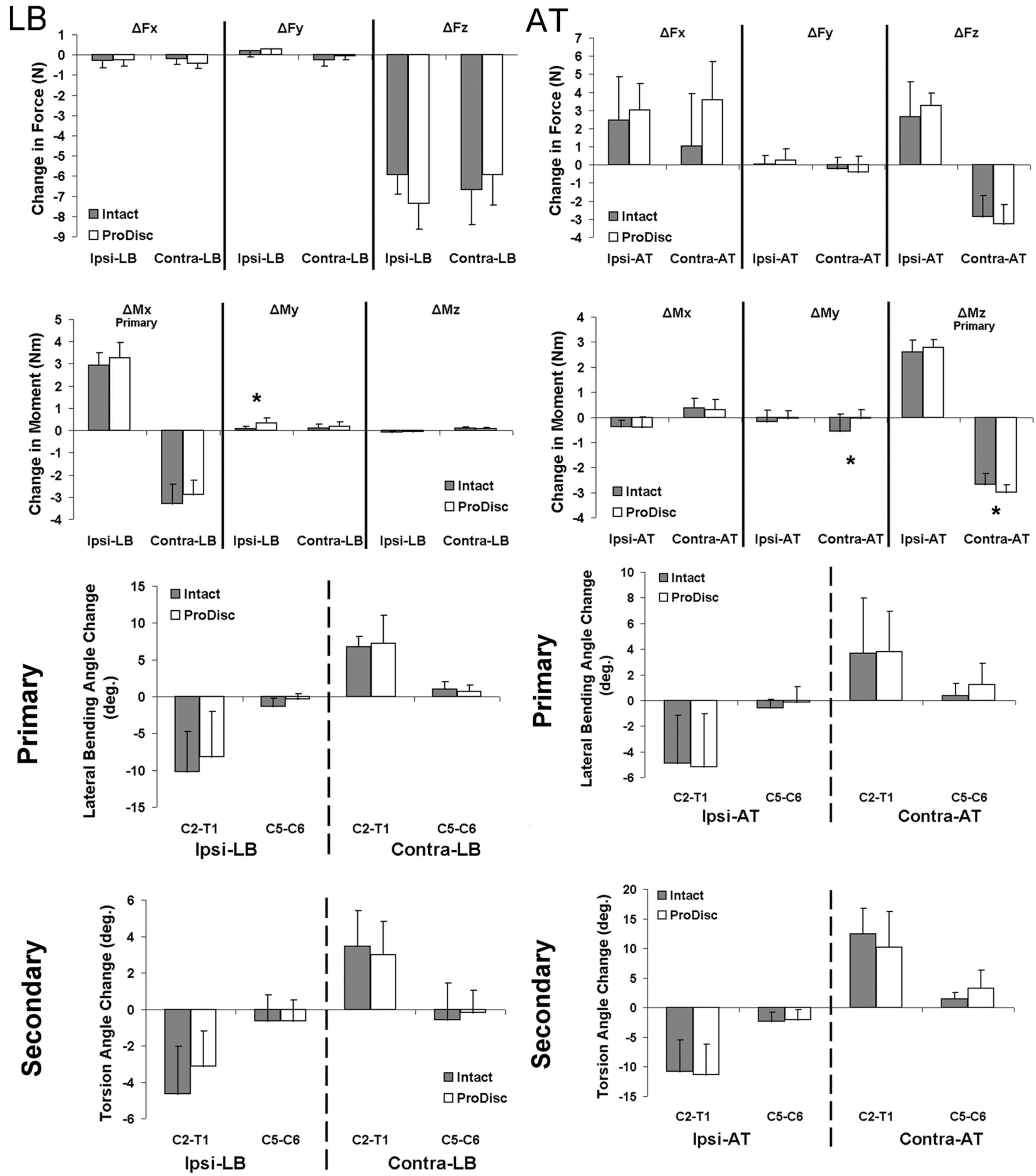

Figure 4. Changes in the forces (ΔF_x, ΔF_y, ΔF_z), the moments (ΔM_x, ΔM_y, ΔM_z), and the primary and coupled angle changes during (LB and AT for the intact and implanted conditions (ProDisc) in both directions of loading. The asterisk (*) indicates a significant difference between the intact and implanted conditions. LB indicates lateral bending; AT, axial torsion.

contralateral lateral bending; in torsion, the change in primary global angle ($\Delta\theta_{G\text{-}AT}$) was also similar between the intact and implanted conditions for both directions. There was no difference between the ipsilateral and contralateral primary global angle ($\Delta\theta_G$) for each condition in both lateral bending and axial torsion (Figure 4; Table 1). The changes in primary segmental angle ($\Delta\theta_S$) were similar between both conditions in each direction of each loading mode. These changes ranged

TABLE 1. Average ± SD Changes in Forces, Moments, Primary and Secondary Global and Segmental Angles, Secondary-to-Primary Moment and Angle Ratios, and Facet Contact Pressure During Lateral Bending and Axial Torsion for the Intact and Implanted Conditions in the Ipsi- and Contralateral Directions

Loading	Condition and Direction	ΔF_x (N)	ΔM_x (N·m)	ΔF_y (N)	ΔM_y (N·m)	ΔF_z (N)	ΔM_z (N·m)	$\Delta M_z/\Delta M_x$ (%)	$\Delta M_x/\Delta M_z$ (%)	$\Delta\theta_G$ (°)		$\Delta\theta_S$ (°)		$\Delta\theta_{G\text{-}AT}/\Delta\theta_{G\text{-}LB}$ (%)	$\Delta\theta_{G\text{-}LB}/\Delta\theta_{G\text{-}AT}$ (%)	$\Delta\theta_{S\text{-}AT}/\Delta\theta_{S\text{-}LB}$ (%)	$\Delta\theta_{S\text{-}LB}/\Delta\theta_{S\text{-}AT}$ (%)	ΔPressure (kPa)
										LB	AT	LB	AT					
Lateral bending	Intact—Ipsi	**− 0.3** ± 0.4	**2.9** ± 0.6	**0.2** ± 0.3	**0.1** ± 0.1	**− 5.9** ± 1.0	**− 0.1** ± 0.0	**− 2.5** ± 1.3	N/A	**− 10.2** ± 5.4	**− 4.6** ± 2.6	**−1.3** ± 1.1	**− 0.6** ± 1.4	**45** ± 14	N/A	**402** ± 898	N/A	**33** ± 23
	ProDisc—Ipsi	**− 0.2** ± 0.3	**3.3** ± 0.7	**0.3** ± 0.3	**0.3** ± 0.2	**− 7.3** ± 1.3	**− 0.1** ± 0.0	**− 1.5** ± 1.3		**− 8.2** ± 6.2	**− 3.1** ± 1.9	**−0.3** ± 0.7	**− 0.6** ± 1.1	**35** ± 46		**− 26** ± 175		**155** ± 136
	Intact—Contra	**− 0.2** ± 0.3	**− 3.3** ± 0.9	**−0.2** ± 0.3	**0.1** ± 0.2	**− 6.7** ± 1.7	**0.1** ± 0.0	**− 3.3** ± 1.0		**6.7** ± 1.4	**3.4** ± 2.0	**1.0** ± 1.0	**− 0.6** ± 2.0	**48** ± 24		**− 155** ± 329		**− 4** ± 3
	ProDisc—Contra	**− 0.4** ± 0.3	**− 2.9** ± 0.6	**0.0** ± 0.2	**0.2** ± 0.2	**− 5.9** ± 1.5	**0.1** ± 0.0	**− 2.8** ± 1.2		**7.2** ± 3.8	**3.0** ± 1.9	**0.7** ± 0.9	**− 0.2** ± 1.2	**77** ± 91		**31** ± 114		**− 12** ± 9
Axial torsion	Intact—Ipsi	**2.4** ± 2.4	**− 0.4** ± 0.2	**0.0** ± 0.4	**− 0.2** ± 0.4	**2.7** ± 1.9	**2.6** ± 0.5	N/A	**− 14.2** ± 10.6	**− 4.9** ± 3.7	**− 10.8** ± 5.3	**− 0.6** ± 0.7	**− 2.3** ± 1.5	N/A	**41** ± 15	N/A	**32** ± 36	**− 18** ± 27
	ProDisc—Ipsi	**3.0** ± 1.5	**− 0.4** ± 0.4	**0.2** ± 0.6	**0.0** ± 0.3	**3.3** ± 0.7	**2.8** ± 0.3		**− 13.3** ± 14.2	**− 5.2** ± 4.1	**− 11.3** ± 5.1	**− 0.1** ± 1.2	**− 2.0** ± 1.7		43 ± 24		− 37 ± 148	47 ± 122
	Intact—Contra	**1.0** ± 2.9	**0.4** ± 0.4	**− 0.2** ± 0.6	**− 0.6** ± 0.7	**− 2.9** ± 1.2	**− 2.7** ± 0.4		**− 15.2** ± 16.6	**3.7** ± 4.3	**12.4** ± 4.4	**0.4** ± 0.9	**1.5** ± 1.1		**26** ± 23		**21** ± 76	**45** ± 48
	ProDisc—Contra	**3.6** ± 2.1	**0.3** ± 0.4	**− 0.4** ± 0.9	**0.0** ± 0.3	**− 3.3** ± 1.1	**− 3.0** ± 0.3		**− 10.1** ± 12.9	**3.8** ± 3.2	**10.2** ± 6.1	**1.2** ± 1.6	**3.3** ± 3.0		**28** ± 23		**73** ± 285	**135** ± 156

Bold values are averages.

LB indicates lateral bending; AT, axial torsion.

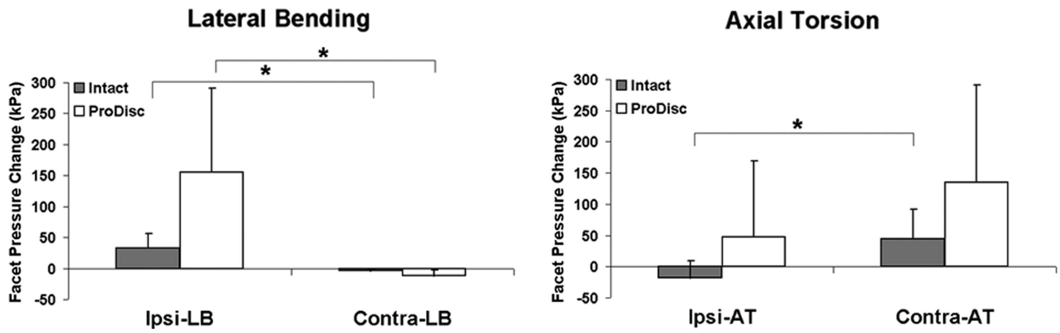

Figure 5. Changes in pressure during LB and AT for the intact and implanted (ProDisc) conditions in both directions of loading. The asterisk (*) indicates a significant difference in pressure between the ipsilateral and contralateral loading directions. LB indicates lateral bending; AT, axial torsion.

between −3.1° and 2.7° in lateral bending and −4.6° and 7.3° in torsion (Figure 4; Table 1).

In the intact condition, the change in primary global angle was significantly greater than the change in coupled global angle in both directions for lateral bending ($P \leq 0.007$, power = 69.6% for ipsilateral and 94.7% for contralateral) and for torsion ($P \leq 0.0004$, power = 67.5% for ipsilateral and 96.3% for contralateral). However, the changes in primary and coupled segmental angles were not different between any loading cases (statistical power ranging from 18% to 53.5%) except in ipsilateral torsion ($P = 0.012$, power = 77.6%). Similarly, in the implanted condition, the change in primary global angle was significantly greater than the change in coupled global angle in both directions for torsion ($P \leq 0.01$, power >69.1%) and in ipsilateral lateral bending ($P = 0.048$, power = 54.8%). Yet, the changes in primary and coupled segmental angles for lateral bending and axial torsion were not different in either loading direction (Figure 4; Table 1).

The ratios of coupled-to-primary global angles were not different between the intact and implanted conditions in the ipsilateral and contralateral directions for each of lateral bending and axial torsion (Table 1). In addition, these ratios were not different between the ipsilateral and contralateral directions of loading, for each of the intact and implanted conditions, in both loading modes. The same relationships were observed for the ratios of coupled-to-primary segmental angles (Table 1).

Facet contact pressure was not greater in the implanted than in the intact condition during both lateral bending and axial torsion (Figure 5; Table 1). During ipsilateral lateral bending, facet contact pressure increased by 33 ± 23 kPa in intact specimens and by 155 ± 136 kPa after implantation (Figure 5; Table 1). In contrast, in contralateral lateral bending, ΔP decreased by 4 ± 3 kPa and 12 ± 9 kPa in the intact and implanted conditions, respectively (Figure 5; Table 1). Although changes in contact pressure were not different between the intact and implanted conditions, they were significantly different between ipsilateral and contralateral lateral bending for the intact ($P = 0.006$, power = 99%) and implanted ($P = 0.007$, power = 90%) conditions (Figure 5). During ipsilateral torsion, facet pressure decreased by 18 ± 27 kPa in the intact condition but increased by 47 ± 122 kPa in the implanted condition (Figure 5; Table 1). However, during contralateral torsion away from the left C5–C6 facet joint, ΔP increased in both the intact (45 ± 48 kPa) and implanted (135 ± 156 kPa) conditions (Figure 5; Table 1). These changes in pressure were not different between the intact and implanted conditions but were significantly different ($P = 0.01$, power = 86%) between ipsilateral and contralateral torsion for the intact condition (Figure 5).

DISCUSSION

Despite a growing clinical interest in local facet joint biomechanics, this is the first study to quantify facet contact pressure in human cadaveric cervical spines in lateral bending and axial torsion in normal loading or in the context of disc arthroplasty. Facet contact pressure at C5–C6 was found to increase, but not significantly, after disc implantation although the rotations in the coronal and axial planes remained unchanged (Figures 4 and 5; Table 1). Although the mean pressures increased, the facet contact pressures exhibited a great deal of variation in the implanted condition (Figure 5; Table 1), which may be the reason for the lack of significant difference. Although degeneration of spinal tissues occurs naturally with aging, this study controlled the degree of C5–C6 disc degeneration and capsule calcification by controlling the selection of specimens, and so the variation in facet pressure measurements are likely not age-dependent. Because this study used a select group of specimens, these findings must be extrapolated cautiously as they do not fully represent all patients, especially because degenerative disease is common with aging. Nonetheless, we eliminated the potential influence of degeneration on facet pressure by evaluating specimens with no evidence of moderate or severe spinal degeneration. Also, both the size and position of the implant could influence the facet pressure measurements. However, in this study, the positioning of the artificial disc was confirmed as appropriate and consistent across specimens. Based on prior work with this facet pressure measurement approach,[54,57] great care was taken to place the probe in the region of greatest contact within the joint, and its placement was the same for both the intact and implanted conditions. Nonetheless, the transducer placement might not have been optimal for these complicated modes of loading.

The variation in pressure observed after disc implantation in both loading modes is likely due to a combination of factors including facet gap opening and a decrease in facet overlap, which have been reported to occur after disc arthroplasty.[62] A recent study using ovine cervical spines reported no change in either the mean or the peak facet pressures after disc arthroplasty subjected to similar moments in lateral bending and torsion.[20] However, that study reported much larger mean pressures (range, 250–270 kPa) than were detected here but used a saddle-shaped implant and a pressure measurement technique that required the joint capsule be transected.[20] We have previously demonstrated that capsule transection alters rotations and contact pressures.[63]

Because of the small number of specimens in this study, the statistical power for comparing facet pressures between the intact and implanted conditions is low in both the lateral bending (ipsilateral 65%; contralateral 61%) and axial torsion (ipsilateral 28%; contralateral 31%) conditions. However, the similarity in the contact pressures in the intact and implanted facet conditions (Figure 5) agrees with facet contact force patterns predicted at C4–C5 in a computational model of a C3–C7 spine under similar magnitudes of lateral bending and axial torsion with a ProDisc-C.[56] In contrast, other computational models predict the location of articular contact to change and the facet force to increase after implantation of a lumbar disc implant under much greater applied lateral bending and torsion moments.[64,65] The effect of disc arthroplasty on facet loading in the lumbar and cervical spines is expected to be different because the anatomy and biomechanics of the facet joints and spine and loading are also different between these spinal regions.

The working biomechanical model of the spinal facet postulates that lateral bending opens the contralateral facet joint and closes, or compresses, the ipsilateral joint, and that axial torsion unloads the ipsilateral facet while loading the contralateral joint.[66,67] Although finite element modeling has also supported this assertion,[56,65,68] this is the first study to quantitatively document this presumed facet joint behavior in both the intact and implanted conditions. Specifically, the contact pressure in the left C5–C6 facet during ipsilateral lateral bending of the cervical spine was significantly increased over contralateral bending in both conditions (Figure 5; Table 1). Furthermore, the C5–C6 facet pressure was greater during contralateral torsion than during ipsilateral torsion (Figure 5; Table 1) in the intact condition only.

The global and segmental rotations for the ball-in-socket disc ProDisc-C are different from those reported for a bi-saddle–shaped artificial disc implant in which rotations decreased by 40% and 26% in lateral bending and axial torsion, respectively.[69] The discrepancy further highlights that the geometry and mechanical designs of the artificial discs affect the vertebral mechanics.[38,48,62,70,71] In addition, both the global (C2–T1) and segmental (C5–C6) primary and coupled rotations measured during lateral bending and axial torsion were unchanged by implantation (Figure 4; Table 1). These findings agree with kinematic data from cadaveric, clinical, and computational studies before and after cervical disc arthroplasty.[48,72,73] For instance, a finite element model of a C5–C6 motion segment under a similar moment in both lateral bending and torsion predicted no change in primary and coupled rotations or facet forces after implantation.[48]

Although the pressure transducer technique used in this study measures only focal contact pressure, it provides accurate and continuous monitoring of contact pressure during spinal loading without altering the biomechanics of the facet joint.[26,54,57,63] Such data can inform on both the magnitude and the temporal pattern of facet contact pressure in the context of spinal kinematics and other local cartilage properties to provide a more comprehensive understanding of the changes in facet joint biomechanics for disc arthroplasty or other spinal intervention. The implantation of a ProDisc-C at the C5–C6 level did not alter the kinematics or the facet pressure in cadaveric cervical spines under physiological lateral bending or axial torsion. Furthermore, this study shows that such a technique can be used to measure contact pressure in more complicated spinal motions and loading scenarios in the context of disc spinal surgical interventions, trauma, and/or pathology.

➢ Key Points

- ❑ Primary and coupled rotations in lateral bending and torsion are similar before and after a single-level ProDisc-C arthroplasty in the lower cervical spine.
- ❑ Facet contact pressure in the posterior region of the cervical facet joint is not increased during lateral bending and axial torsion after ProDisc-C arthroplasty at the same level.
- ❑ Facet contact pressure is significantly greater in the joint ipsilateral to the applied lateral bending than in the contralateral joint in both the intact and implanted conditions.
- ❑ Facet contact pressure is significantly greater in the joint contralateral to the directed axial torsion in the intact case only.

References

1. Bogduk N, Mercer S. Biomechanics of the cervical spine. I: normal kinematics. *Clin Biomech* 2000;15:633–48.
2. Panjabi MM, Crisco JJ, Vasavada A, et al. Mechanical properties of the human cervical spine as shown by three-dimensional load-displacement curves. *Spine* 2001;26:2692–700.
3. Winkelstein BA, Myers BS. Experimental and computational characterization of three-dimensional cervical spine flexibility. *Stapp Car Crash J* 2000;44:139–58.
4. Winkelstein BA, Myers BS. Importance of nonlinear and multivariable flexibility coefficients in the prediction of human cervical spine motion. *J Biomech Eng* 2002;124:504–11.
5. Siegmund GP, Davis MB, Quinn KP, et al. Head-turned postures increase the risk of cervical facet capsule injury during whiplash. *Spine* 2008;33:1643–49.
6. Lysell E. Motion in the cervical spine. An experimental study on autopsy specimens. *Acta Orthop Scand* 1969;(suppl 123):1+.
7. Milne N. The role of zygapophysial joint orientation and uncinate processes in controlling motion in the cervical spine. *J Anat* 1991;178:189–201.

8. Panjabi MM, Oxland T, Takata K, et al. Articular facets of the human spine. Quantitative three-dimensional anatomy. *Spine* 1993;18:1298–310.
9. Onan OA, Heggeness MH, Hipp JA. A motion analysis of the cervical facet joint. *Spine* 1998;23:430–9.
10. Haher TR, O'Brien M, Dryer JW, et al. The role of the lumbar facet joints in spinal stability. Identification of alternative paths of loading. *Spine* 1994;19:2667–71.
11. Onan OA, Hipp JA, Heggeness MH. Use of computed tomography image processing for mapping of human cervical facet surface geometry. *Med Eng Phys* 1998;20:77–81.
12. Hsu WH, Benzel EC, Chen TY, et al. Axial and coronal orientation of subaxial cervical zygapophysial joints and their effect on axial rotation and lateral bending. *Spine* 2008;33:2409–14.
13. Raynor RB, Moskovich R, Zidel P, et al. Alterations in primary and coupled neck motions after facetectomy. *Neurosurgery* 1987;21:681–7.
14. Clausen JD, Goel VK, Traynelis VC, et al. Uncinate processes and Luschka joints influence the biomechanics of the cervical spine: quantification using a finite element model of the C5-C6 segment. *J Orthop Res* 1997;15:342–7.
15. Ng HW, Teo EC, Lee KK, et al. Finite element analysis of cervical spinal instability under physiologic loading. *J Spinal Disord Tech* 2003;16:55–65.
16. Adams MA, Hutton WC. The effect of posture on the role of the apophysial joints in resisting intervertebral compressive forces. *J Bone Joint Surg Br* 1980;62:358–62.
17. Yang KH, King AI. Mechanism of facet load transmission as a hypothesis for low-back pain. *Spine* 1984;9:557–65.
18. Sawa AG, Crawford NR. The use of surface strain data and a neural networks solution method to determine lumbar facet joint loads during in vitro spine testing. *J Biomech* 2008;41:2647–53.
19. Schmidt H, Heuer F, Wilke HJ. Interaction between finite helical axes and facet joint forces under combined loading. *Spine* 2008;33:2741–8.
20. Stieber JR, Quirno M, Kang M, et al. The facet joint loading profile of a cervical intervertebral disc replacement incorporating a novel saddle-shaped articulation. *J Spinal Disord Tech* 2011;24:432–6.
21. Butler D, Trafimow JH, Andersson GB, et al. Discs degenerate before facets. *Spine* 1990;15:111–3.
22. Dunlop RB, Adams M A, Hutton WC. Disc space narrowing and the lumbar facet joints. *J Bone Joint Surg Br* 1984;66:706–10.
23. Kumaresan S, Yoganandan N, Pintar FA. Finite element modeling approaches of human cervical spine facet joint capsule. *J Biomech* 1998;31:371–6.
24. Fujiwara A, Tamai K, Yamato M, et al. The relationship between facet joint osteoarthritis and disc degeneration of the lumbar spine: an MRI study. *Eur Spine J* 1999;8:396–401.
25. Ingalhalikar AV, Reddy CG, Lim TH, et al. Effect of lumbar total disc arthroplasty on the segmental motion and intradiscal pressure at the adjacent level: an in vitro biomechanical study: presented at the 2008 Joint Spine Section Meeting Laboratory investigation. *J Neurosurg Spine* 2009;11:715–23.
26. Jaumard NV, Bauman JA, Welch WC, et al. Pressure measurement in the cervical spinal facet joint: considerations for maintaining joint anatomy and an intact capsule. *Spine* 2011;36:1197–203.
27. Liu YK, Goel VK, Dejong A, et al. Torsional fatigue of the lumbar intervertebral joints. *Spine* 1985;10:894–900.
28. Jeffrey JE, Gregory DW, Aspden RM. Matrix damage and chondrocyte viability following a single impact load on articular cartilage. *Arch Biochem Biophys* 1995;322:87–96.
29. Kurz B, Jin M, Patwari P, et al. Biosynthetic response and mechanical properties of articular cartilage after injurious compression. *J Orthop Res* 2001;19:1140–6.
30. Morel V, Merçay A, Quinn TM. Prestrain decreases cartilage susceptibility to injury by ramp compression in vitro. *Osteoarthritis Cartilage* 2005;13:964–70.
31. Knecht S, Vanwanseele B, Stüssi E. A review on the mechanical quality of articular cartilage: implications for the diagnosis of osteoarthritis. *Clin Biomech* 2006;21:999–1012.
32. Isaac DI, Meyer EG, Haut RC. Chondrocyte damage and contact pressures following impact on the rabbit tibiofemoral joint. *J Biomech Eng* 2008;130:041018.
33. Natoli RM, Scott CC, Athanasiou KA. Temporal effects of impact on articular cartilage cell death, gene expression, matrix biochemistry, and biomechanics. *Ann Biomed Eng* 2008;36:780–92.
34. Schmidt H, Heuer F, Claes L, et al. The relation between the instantaneous center of rotation and facet joint forces—A finite element analysis. *Clin Biomech* 2008;23:270–8.
35. Cunningham BW, Hu N, Zorn CM, et al. Biomechanical comparison of single- and two-level cervical arthroplasty versus arthrodesis: effect on adjacent-level spinal kinematics. *Spine J* 2010;10:341–9.
36. SariAli el-H, Lemaire JP, Pascal-Mousselard H, et al. In vivo study of the kinematics in axial rotation of the lumbar spine after total intervertebral disc replacement: long-term results: a 10–14 years follow up evaluation. *Eur Spine J* 2006;15:1501–10.
37. Demetropoulos CK, Sengupta DK, Knaub MA, et al. Biomechanical evaluation of the kinematics of the cadaver lumbar spine following disc replacement with the ProDisc-L prosthesis. *Spine* 2010;35:26–31.
38. Lazaro BC, Yucesoy K, Yuksel KZ, et al. Effect of arthroplasty design on cervical spine kinematics: analysis of the Bryan Disc, ProDisc-C, and Synergy disc. *Neurosurg Focus* 2010;28:E6.
39. Duggal N, Bertagnoli R, Rabin D, et al. ProDisc-C: an in vivo kinematic study. *J Spinal Disord Tech* 2011;24:334–9.
40. Kowalczyk I, Lazaro BC, Fink M, et al. Analysis of in vivo kinematics of 3 different cervical devices: Bryan disc, ProDisc-C, and Prestige LP disc. *J Neurosurg Spine* 2011;15:630–5.
41. Shim CS, Lee SH, Shin HD, et al. CHARITE versus ProDisc: a comparative study of a minimum 3-year follow-up. *Spine* 2007;32:1012–8.
42. Siepe CJ, Korge A, Grochulla F, et al. Analysis of post-operative pain patterns following total lumbar disc replacement: results from fluoroscopically guided spine infiltrations. *Eur Spine J* 2008;17:44–56.
43. Ryu KS, Park CK, Jun SC, et al. Radiological changes of the operated and adjacent segments following cervical arthroplasty after a minimum 24-month follow-up: comparison between the Bryan and Prodisc-C devices. *J Neurosurg Spine* 2010;13:299–307.
44. Wininger KL, Deshpande KK, Bester ML. Persistent pain following lumbar disc replacement. *Radiol Technol* 2012;83:430–6.
45. Dooris AP, Goel VK, Grosland NM, et al. Load-sharing between anterior and posterior elements in a lumbar motion segment implanted with an artificial disc. *Spine* 2001;26:E122–9.
46. Rousseau MA, Bradford DS, Bertagnoli R, et al. Disc arthroplasty design influences intervertebral kinematics and facet forces. *Eur Spine J* 2006;6:258–66.
47. Chang UK, Kim DH, Lee MC, et al. Changes in adjacent-level disc pressure and facet joint force after cervical arthroplasty compared with cervical discectomy and fusion. *J Neurosurg Spine* 2007;7:33–9.
48. Rousseau MA, Bonnet X, Skalli W. Influence of the geometry of a ball-and-socket intervertebral prosthesis at the cervical spine: a finite element study. *Spine* 2008;33:E10–4.
49. Rundell SA, Auerbach JD, Balderston RA, et al. Total disc replacement positioning affects facet contact forces and vertebral body strains. *Spine* 2008;33:2510–17.
50. Rohlmann A, Mann A, Zander T, et al. Effect of an artificial disc on lumbar spine biomechanics: a probabilistic finite element study. *Eur Spine J* 2009;18:89–97.
51. Zander T, Rohlmann A, Bergmann G. Influence of different artificial disc kinematics on spine biomechanics. *Clin Biomech* 2009;24:135–42.
52. Kang H, Park P, La Marca F, et al. Analysis of load sharing on uncovertebral and facet joints at the c5–6 level with implantation of the Bryan, Prestige LP, or Prodisc-C cervical disc prosthesis: an in vivo image-based finite element study. *Neurosurg Focus* 2010;28:E9.
53. Galbusera F, Anasetti F, Bellini CM, et al. The influence of the axial, antero-posterior and lateral positions of the center of rotation of a ball-and-socket disc prosthesis on the cervical spine biomechanics. *Clin Biomech* 2010;25:397–401.

54. Bauman JA, Jaumard NV, Guarino BB, et al. Facet joint contact pressure is not significantly affected by ProDisc cervical disc arthroplasty in sagittal bending: a single level cadaveric study. *Spine J* 2012;12:949–59.
55. Chen W-M, Park CK, Lee KY. In situ contact analysis of the prosthesis components of ProDisc-L in lumbar spine following total disc replacement. *Spine* 2009;34:E716–23.
56. Womack W, Leahy PD, Patel VV, et al. Finite element modeling of kinematic and load transmission alterations due to cervical intervertebral disc replacement. *Spine* 2011;36:E1126–33.
57. Jaumard NV, Bauman JA, Weisshaar CL, et al. Contact pressure in the facet joint during sagittal bending of the cadaveric cervical spine. *J Biomech Eng* 2011;133:071004.
58. Frobin W, Leivseth G, Biggemann M, et al. Vertebral height, disc height, posteroanterior displacement and dens-atlas gap in the cervical spine: precision measurement protocol and normal data. *Clin Biomech* 2002;17:423–31.
59. Kettler A, Rohlmann F, Neidlinger-Wilke C, et al. Validity and interobserver agreement of a new radiographic grading system for intervertebral disc degeneration: part II. Cervical spine. *Eur Spine J* 2006;15:732–41.
60. McAfee PC, Cunningham BW, Hayes V, et al. Biomechanical analysis of rotational motions after disc arthroplasty: implications for patients with adult deformities. *Spine* 2006;31(suppl): S152–60.
61. Galbusera F, Bellini CM, Raimondi MT, et al. Cervical spine biomechanics following implantation of a disc prosthesis. *Med Eng Phys* 2008;30:1127–33.
62. Liu J, Ebraheim NA, Haman SP, et al. How the increase of the cervical disc space height affects the facet joint: an anatomy study. *Spine* 2006;31:E350–4.
63. Jaumard NV, Bauman JA, Welch WC, et al. Biomechanical comparison of contact pressure in the cervical facet joint during bending using a probe and pressure-sensitive paper. Paper presented at: ASME Summer Bioengineering Conference; June 2010; Naples, FL. Article 19498.
64. Rohlmann A, Zander T, Bock B, et al. Effect of position and height of a mobile core type artificial disc on the biomechanical behaviour of the lumbar spine. *Proc Inst Mech Eng H* 2008;222:229–39.
65. Schmidt H, Midderhoff S, Adkins K, et al. The effect of different design concepts in lumbar total disc arthroplasty on the range of motion, facet joint forces and instantaneous center of rotation of a L4–5 segment. *Eur Spine J* 2009;18:1695–705.
66. Schafer RC. Cervical spine. In: Motion Palpation Institute. 2nd ed. *Motion Palpation and Chiropractic Technique: Principles Dynamic Chiropractic*. Arlington, VA: ACA Press; 1990.
67. Buttermann GR, Kahmann RD, Lewis JL, et al. An experimental method for measuring force on the spinal facet joint: description and application of the method. *J Biomech Eng* 1991;113:375–86.
68. Kuo CS, Hu HT, Lin RM, et al. Biomechanical analysis of the lumbar spine on facet joint force and intradiscal pressure—a finite element study. *BMC Musculoskelet Disord* 2010;11:151.
69. Finn MA, Brodke DS, Daubs M, et al. Local and global subaxial cervical spine biomechanics after single-level fusion or cervical arthroplasty. *Eur Spine J* 2009;18:1520–7.
70. Lin CY, Kang H, Rouleau JP, et al. Stress analysis of the interface between cervical vertebrae end plates and the Bryan, Prestige LP, and ProDisc-C cervical disc prostheses: an in vivo image-based finite element study. *Spine* 2009;34:1554–60.
71. Lee SH, Im YJ, Kim KT, et al. Comparison of cervical spine biomechanics after fixed- and mobile-core artificial disc replacement: a finite element analysis. *Spine* 2011;36:700–8.
72. DiAngelo DJ, Foley KT, Morrow BR, et al. In vitro biomechanics of cervical disc arthroplasty with the ProDisc-C total disc implant. *Neurosurg Focus* 2004;17:E7.
73. Park JJ, Quirno M, Cunningham MR, et al. Analysis of segmental cervical spine vertebral motion after prodisc-C cervical disc replacement. *Spine* 2010;35:E285–9.